Supplemental Materials to

In silico investigation of the clinical translatability of competitive clearance glucose-responsive insulins

Jing Fan Yang[1], Sungyun Yang[1], Xun Gong[1], Naveed A. Bakh[1], Ge Zhang[1], Allison B. Wang[1], Alan D. Cherrington[2], Michael A. Weiss[3], and Michael S. Strano[1]*

[1]Department of Chemical Engineering, Massachusetts Institute of Technology, MA 02139, USA.

[2]Molecular Physiology and Biophysics, Vanderbilt University School of Medicine, TN 37232, USA

[3]Department of Biochemistry & Molecular Biology, Indiana University School of Medicine, IN 46202, USA

*: Corresponding author: Michael S. Strano (strano@mit.edu)

S1. Mathematical Model Setup

Table S1. Physiological parameters for minipigs and humans based on *a priori* experimental measurements published in the literature or by the vendor.

	Physiological Parameter	Minipig	Human	Unit	Physiological Parameter	Rats	Mice	Unit
	Bodyweight	36	70	[kg]				
Volumes of Compartments[a]	$V^{G}_{brain,v}$	5.25E-1	1.69E-04	[dL]	V^{I}_{brain}	3.55E-2	1.21E-05	[L]
	$V^{G}_{brain,i}$	1.31E-1	1.07E-03					
	V^{G}_{heart}	5.83	5.79E-03		V^{I}_{heart}	2.95E-1	4.14E-04	
	V^{G}_{liver}	8.62	1.78E-02		V^{I}_{liver}	3.16E-1	6.86E-04	
	V^{G}_{gut}	6.13	8.26E-03		V^{I}_{gut}	5.31E-1	7.43E-04	
	$V^{G}_{kidneys}$	2.00	2.93E-03		$V^{I}_{kidneys}$	1.44E-1	2.43E-04	
	$V^{G}_{periphery,v}$	5.95	5.20E-03		$V^{I}_{periphery,v}$	4.03E-2	3.72E-04	
	$V^{G}_{periphery,i}$	2.69E1	1.62E-02		$V^{I}_{periphery,i}$	2.69	1.62E-03	
Blood Flow Rates[a]	Q^{G}_{brain}	1.97	8.88E-04	[dL/min]	Q^{I}_{brain}	1.33E-1	6.35E-05	[L/min]
	Q^{G}_{heart}	3.68E1	5.12E-02		Q^{I}_{heart}	2.49	3.66E-03	
	Q^{G}_{liver}	1.01E1	1.73E-02		Q^{I}_{liver}	6.85E-1	1.24E-03	
	Q^{G}_{gut}	8.85	1.47E-02		Q^{I}_{gut}	5.99E-1	1.05E-03	
	Q^{G}_{kidney}	6.56	9.21E-03		Q^{I}_{kidney}	4.44E-1	6.59E-04	
	$Q^{G}_{periphery}$	1.81E1	2.38E-02		$Q^{I}_{periphery}$	1.23	1.70E-03	
	$Q^{G}_{hepatic\ artery}$	1.27	2.66E-03		$Q^{I}_{hepatic\ artery}$	8.01E-2	1.91E-04	
	$Q_{muscle} / Q_{adipose}$	1.22[b]	2.74	[-]				
TDT[c]	$T^{G}_{periphery}$	4.0	5.0	[min]	$T^{I}_{periphery}$	1.6E1	2.0E1	[min]
	T^{G}_{brain}	1.7	2.1					

[a] Compartmental volumes used in the minipig model are based on systematic measurements done by Sinclair Bio Resources, LLC.[1] Blood flow rates are based on haemodynamics measurements in Wyler *et al*.[2] Values used in the human model are scaled 1.35-fold from those in Sorensen's original publication to match with the intrinsic RHI clearance rate observed in clinical trials.[3,4]

[b] Based on the work of Suenderhauf and Parrott.[5]

[c] TDT, the transcapillary diffusion time between the vascular and interstitial volumes, were scaled by body mass from the human models.

Table S2. Pharmacokinetic parameters for minipigs and humans. Estimated (*Est.*) and distinguishingly parameterized (*Dis.*; *i.e.* separately estimated for the healthy and diabetic populations) variables are marked by circles.

MINIPIGS							
			Diabetic	Healthy	Unit	Est.	Dis.
Hepatic Glucose Uptake	R_{HGU}	=	$R_{\mathrm{HGU}}^{\mathrm{basal}} M_{\mathrm{HGU}}^{\mathrm{G}} M_{\mathrm{HGU}}^{\mathrm{I}}$		[mg/min]		
	$R_{\mathrm{HGU}}^{\mathrm{basal}}$	=	8.01		[mg/min]	○[a]	
	$M_{\mathrm{HGU}}^{\mathrm{G}}$	=	$2.83 + 2.83\tanh\{1.60([\mathrm{G}]_{\mathrm{L,n}} - 1.48)\}$		[-]	○[b]	
	$\frac{dM_{\mathrm{HGU}}^{\mathrm{I}}}{dt}$	=	$(M_{\mathrm{HGU}}^{\mathrm{I}\infty} - M_{\mathrm{HGU}}^{\mathrm{I}}) / \tau_1$		[min^{-1}]		
	$M_{\mathrm{HGU}}^{\mathrm{I}\infty}$	=	$2.00\tanh(0.55[\mathrm{I}]_{\mathrm{L,n}})$		[-]		
	τ_1	=	25		[min]		
Hepatic Glucose Production	R_{HGP}	=	$R_{\mathrm{HGP}}^{\mathrm{basal}} M_{\mathrm{HGP}}^{\mathrm{G}} M_{\mathrm{HGP}}^{\mathrm{I}} M_{\mathrm{HGP}}^{\Gamma}$		[mg/min]		
	$R_{\mathrm{HGP}}^{\mathrm{basal}}$	=	$\sum_{k=\mathrm{H,\,P,\,B,\,RBC,\,G}} R_{k\mathrm{GU}}^{\mathrm{basal}}$		[mg/min]		
	$M_{\mathrm{HGP}}^{\mathrm{G}}$	=	$1.02 - 0.02\tanh\{6.47\,([\mathrm{G}]_{\mathrm{L,n}} - 0.43)\}$	$1.19 - 1.27\tanh\{1.26([\mathrm{G}]_{\mathrm{L,n}} - 0.33)\}$	[-]	○[b]	○
	$\frac{dM_{\mathrm{HGP}}^{\mathrm{I}}}{dt}$	=	$(M_{\mathrm{HGP}}^{\mathrm{I}\infty} - M_{\mathrm{HGP}}^{\mathrm{I}}) / \tau_1$		[min^{-1}]		
	$M_{\mathrm{HGP}}^{\mathrm{I}\infty}$	=	$1.01 - 0.16\tanh\{0.60([\mathrm{I}]_{\mathrm{L,n}} - 0.89)\}$		[-]	○	
	$M_{\mathrm{HGP}}^{\Gamma}$	=	$M_{\mathrm{HGP}}^{\Gamma 0} - f_2$		[-]		
	$M_{\mathrm{HGP}}^{\Gamma 0}$	=	$\tanh\{19.12[\Gamma]_{\mathrm{n}}\}$		[-]	○	
	df_2 / dt	=	$\{(M_{\mathrm{HGP}}^{\Gamma 0} - 1) / 2 - f_2\} / \tau_2$		[min^{-1}]		
	τ_2	=	65		[min]		
Periphery Glucose Uptake	R_{PGU}	=	$R_{\mathrm{PGU}}^{\mathrm{basal}} M_{\mathrm{PGU}}^{\mathrm{G}} M_{\mathrm{PGU}}^{\mathrm{I}}$		[mg/min]		
	$R_{\mathrm{PGU}}^{\mathrm{basal}}$	=	42.88		[mg/min]	○[a]	
	$M_{\mathrm{PGU}}^{\mathrm{G}}$	=	$[\mathrm{G}]_{\mathrm{P,i,n}}$		[-]		
	$M_{\mathrm{PGU}}^{\mathrm{I}}$	=	$8.37 + 9.00\tanh\{0.29([\mathrm{I}]_{\mathrm{P,i,n}} - 4.99)\}$	$18.98 + 18.00\tanh\{0.80([\mathrm{I}]_{\mathrm{P,i,n}} - 5.66)\}$	[-]	○	○
Kidney Glucose Excretion[c]	R_{KGE}	=	$\begin{cases} 71 + 71\tanh[0.11([\mathrm{G}]_{\mathrm{kidney}} - 460)] & \text{if } 0 \le [\mathrm{G}]_{\mathrm{kidney}} < 460\,\mathrm{mg\,dL^{-1}} \\ -330 + 0.872[\mathrm{G}]_{\mathrm{kidney}} & \text{if } [\mathrm{G}]_{\mathrm{kidney}} > 460\ \mathrm{mg\,dL^{-1}} \end{cases}$		[mg/min]		
Kidney Insulin Clearance	R_{KIC}	=	$F_{KIC} Q_K^I I_K$		[mU/min]		
	F_{KIC}	=	3.00E-1		[-]		
Liver Insulin Clearance	R_{LIC}	=	$F_{LIC}(Q_{\mathrm{adipose}}^{\mathrm{I}}[\mathrm{I}]_{\mathrm{heart}} + Q_{\mathrm{gut}}^{\mathrm{I}}[\mathrm{I}]_{\mathrm{gut}})$		[mU/min]		
	F_{LIC}	=	4.00E-1		[-]		
Muscle Insulin Clearance	R_{MIC}	=	$\frac{[\mathrm{I}]_{\mathrm{muscle,i}}}{\frac{1-F_{PIC}}{F_{PIC}}\frac{1}{Q_{\mathrm{muscle}}^{\mathrm{I}}} - \frac{T_{\mathrm{muscle}}^{\mathrm{I}}}{V_{\mathrm{muscle,i}}^{\mathrm{I}}}}$		[mU/min]		
	F_{PIC}	=	2.23E-2	4.21E-2	[-]	○	○
Adipose Insulin Clearance	R_{AIC}	=	$\frac{[\mathrm{I}]_{\mathrm{adipose,i}}}{\frac{1-F_{PIC}}{F_{PIC}}\frac{1}{Q_{\mathrm{adipose}}^{\mathrm{I}}} - \frac{T_{\mathrm{adipose}}^{\mathrm{I}}}{V_{\mathrm{adipose,i}}^{\mathrm{I}}}}$		[mU/min]		
Brain Glucose Uptake	R_{BGU}	=	2.94[c]		[mg/min]		
Red Blood Cell Glucose Uptake	R_{RBCU}	=	4.91[c]		[mg/min]		

Gut Glucose Uptake	R_{GGU}	=	27.08	[mg/min]	○[a]
Subcutaneous Insulin Absorption[d]	$R_{SIA,adipose,i}$	=	$k_{abs}[I_{dm}]_{depot}$	[mU/L/min]	
	$\frac{d[I_{dm}]}{dt}$	=	$k_{h/dm}[I_{hex}] - (k_{abs} + k_{loss})[I_{dm}]$	[mU/L/min]	
	$\frac{d[I_{hex}]}{dt}$	=	$-(k_{h/dm} + k_{loss})[I_{hex}]$	[mU/L/min]	
	RHI k_{abs}	=	4.90E-3	[min^{-1}]	○
	RHI $k_{h/dm}$	=	1.40E-2	[min^{-1}]	○
	k_{loss}	=	$3D_{inj}(3V_{inj}/4\pi)^{-2/3}$	[min^{-1}]	
	D_{inj}	=	9.00E-5	[cm^2/min]	
Parameters Specific to MK-2640[e]	K_G	=	6.8E-3	[mM$^{-h_G}$]	○[f]
	h_G	=	2.5	[-]	○[f]
	K_M	=	3.0[g]	[nM]	
	h_{GRI}	=	1.5	[-]	○[f]
	GRI k_{abs}	=	4.40E-3	[min^{-1}]	○[h]
	GRI $k_{h/dm}$	=	1.40E-2	[min^{-1}]	○[h]

HUMAN						
			Diabetic	Healthy	Unit	
Hepatic Glucose Uptake	R_{HGU}	=	$R_{HGU}^{basal} M_{HGU}^{G} M_{HGU}^{I}$		[mg/min]	
	R_{HGU}^{basal}	=	20		[mg/min]	
	M_{HGU}^{G}	=	$-1.02 + 2.26\tanh\{4.80([G]_{L,n} - 0.70)\}$	$5.66 + 5.66\tanh\{2.44([G]_{L,n} - 1.48)\}$	[-]	○[i]
	$\frac{dM_{HGU}^{I}}{dt}$	=	$(M_{HGU}^{I\infty} - M_{HGU}^{I})/\tau_1$		[min^{-1}]	
	$M_{HGU}^{I\infty}$	=	$2\tanh(0.55[I]_{L,n})$		[-]	
	τ_1	=	25		[min]	
Hepatic Glucose Production	R_{HGP}	=	$R_{HGP}^{basal} M_{HGP}^{G} M_{HGP}^{I} M_{HGP}^{\Gamma}$		[mg/min]	
	R_{HGP}^{basal}	=	$\sum_{k=H,P,B,RBC,G} R_{kGU}^{basal}$		[mg/min]	
	M_{HGP}^{G}	=	$1.42 - 1.41\tanh\{0.62([G]_{L,n} - 0.50)\}$		[-]	
	$\frac{dM_{HGP}^{I}}{dt}$	=	$R_{HGP}^{basal} M_{HGP}^{G} M_{HGP}^{I} M_{HGP}^{\Gamma}$		[min^{-1}]	
	$M_{HGP}^{I\infty}$	=	$1.21 - 1.14\tanh\{1.66([I]_{L,n} - 0.89)\}$		[-]	
	M_{HGP}^{Γ}	=	$M_{HGP}^{\Gamma 0} - f_2$		[-]	
	$M_{HGP}^{\Gamma 0}$	=	$2.7\tanh\{0.39[\Gamma]_n\}$		[-]	
	df_2/dt	=	$\{(M_{HGP}^{\Gamma 0} - 1)/2 - f_2\}/\tau_2$		[min^{-1}]	
	τ_2	=	65		[min]	
Periphery Glucose Uptake	R_{PGU}	=	$R_{PGU}^{basal} M_{PGU}^{G} M_{PGU}^{I}$		[mg/min]	
	R_{PGU}^{basal}	=	40		[mg/min]	
	M_{PGU}^{G}	=	$[G]_{P,i,n}$		[-]	
	M_{PGU}^{I}	=	$7.03 + 6.52\tanh\{0.34([I]_{P,i,n} - 5.82)\}$	$11.00 + 16.96\tanh\{0.07([I]_{P,i,n} - 10.84)\}$	[-]	○[i]
Kidney Glucose Excretion	R_{KGE}	=	$\begin{cases} 71 + 71\tanh[0.11([G]_{kidney} - 460)] & \text{if } 0 \le [G]_{kidney} < 460\ \text{mg dL}^{-1} \\ -330 + 0.872[G]_{kidney} & \text{if } [G]_{kidney} > 460\ \text{mg dL}^{-1} \end{cases}$		[mg/min]	
Kidney Insulin Clearance	R_{KIC}	=	$F_{KIC} Q_K^I I_K$		[mU/min]	
	F_{KIC}	=	3.00E-1		[-]	

Liver Insulin Clearance	R_{LIC}	=	$F_{LIC}(Q^{\mathrm{I}}_{\mathrm{adipose}}[\mathrm{I}]_{\mathrm{heart}} + Q^{\mathrm{I}}_{\mathrm{gut}}[\mathrm{I}]_{\mathrm{gut}})$	[mU/min]	
	F_{LIC}	=	4.00E-1	[-]	
Muscle Insulin Clearance	R_{MIC}	=	$\dfrac{[\mathrm{I}]_{\mathrm{muscle,i}}}{\dfrac{1-F_{PIC}}{F_{PIC}}\dfrac{1}{Q^{\mathrm{I}}_{\mathrm{muscle}}} - \dfrac{T^{\mathrm{I}}_{\mathrm{muscle}}}{V^{\mathrm{I}}_{\mathrm{muscle,i}}}}$	[mU/min]	
	F_{PIC}	=	1.50E-1	[-]	
Adipose Insulin Clearance	R_{AIC}	=	$\dfrac{[\mathrm{I}]_{\mathrm{adipose,i}}}{\dfrac{1-F_{PIC}}{F_{PIC}}\dfrac{1}{Q^{\mathrm{I}}_{\mathrm{adipose}}} - \dfrac{T^{\mathrm{I}}_{\mathrm{adipose}}}{V^{\mathrm{I}}_{\mathrm{adipose,i}}}}$	[mU/min]	
Brain Glucose Uptake	R_{BGU}	=	70	[mg/min]	
Red Blood Cell Glucose Uptake	R_{RBCU}	=	10	[mg/min]	
Gut Glucose Uptake	R_{GGU}	=	20	[mg/min]	
Subcutaneous Insulin Absorption[d]	$R_{\mathrm{SIA,adipose,i}}$	=	$k_{\mathrm{abs}}[\mathrm{I}_{\mathrm{dm}}]_{\mathrm{depot}}$	[mU/L/min]	
	$\dfrac{d[\mathrm{I}_{\mathrm{dm}}]}{dt}$	=	$k_{\mathrm{h/dm}}[\mathrm{I}_{\mathrm{hex}}] - (k_{\mathrm{abs}} + k_{\mathrm{loss}})[\mathrm{I}_{\mathrm{dm}}]$	[mU/L/min]	
	$\dfrac{d[\mathrm{I}_{\mathrm{hex}}]}{dt}$	=	$-(k_{\mathrm{h/dm}} + k_{\mathrm{loss}})[\mathrm{I}_{\mathrm{hex}}]$	[mU/L/min]	
	RHI k_{abs}	=	8.90E-03	[min^{-1}]	
	$k_{\mathrm{h/dm}}$	=	5.65E-02	[min^{-1}]	
	k_{loss}	=	$3D_{\mathrm{inj}}(3V_{\mathrm{inj}}/4\pi)^{-2/3}$	[min^{-1}]	
	D_{inj}	=	9.00E-5	[cm^2/min]	
Parameters Specific to MK-2640[e, j]	K_{G}	=	1.1E-3	[mM$^{-h_{\mathrm{G}}}$]	○[f]
	h_{G}	=	2.5	[-]	○[f]
	K_{M}	=	3.4[g]	[nM]	
	h_{GRI}	=	1.5	[-]	○[f]

[a] Estimated from literature-based initial guesses.[6-8]

[b] $[\mathrm{G}]_{k,\mathrm{n}}$,$[\mathrm{I}]_{k,\mathrm{n}}$, and $[\Gamma]_{\mathrm{n}}$ denote glucose, insulin, and glucagon concentrations normalized by the steady state levels, where k denotes the corresponding compartment. Naturally, all multipliers (M) should assume a value of 1 for a normalized concentration of 1.

[c] Based on measurements previously reported in the literature.[9,10]

[d] Simulation of the subcutaneous injection depot follows the work by Bakh *et al.*,[11] which in turn was based on Wong *et al.*[12,13] This model assumes an equilibrium between hexameric insulin and dimeric/monomeric insulins. The latter are absorbed from the injection depot into circulation at a rate dictated by k_{abs}.

[e] Excluding the parameter values already shown in Table 1 of the Main Text.

[f] See Research Design and Methods.

[g] Directly measured experimentally by Kaarsholm *et al*.[14]

[h] MK-2640's subcutaneous injection rate constants in minipigs were estimated from the diabetic subcutaneous injection data reported in Kaarsholm *et al*.[14]

[i] Expressions of $\mathrm{M}^{\mathrm{G}}_{\mathrm{HGU}}$ in diabetic humans and $\mathrm{M}^{\mathrm{I}}_{\mathrm{PGU}}$ in non-diabetic humans were adjusted to match the clinical results. Previously in the original Sorensen report,[3] $\mathrm{M}^{\mathrm{G}}_{\mathrm{HGU}}$ was only parameterized with measurements on healthy individuals and $\mathrm{M}^{\mathrm{I}}_{\mathrm{PGU}}$, diabetic patients. Their respective application to diabetic and healthy humans, therefore, called for refinement with the most recent data with matching health conditions.

[j] MK-2640's k_{abs} and $k_{\mathrm{h/dm}}$ in humans are unavailable since no subcutaneous clinical data were published.

S2. Mathematical Treatment of MK-2640's Reduced IR Affinity

The physiological model component of IM^{3}PACT was established for describing the interplay among glucose, glucagon, and regular human insulin (RHI). For the two-state GRI design studied in our previous work,[15] the dormant form was assumed to be triggered by the presence of glucose to become the activated form indistinguishable from an endogenous RHI molecule. MK-2640, however, is known to be significantly less potent on the molecular scale relative to RHI due to its weak binding to insulin receptors. As briefly mentioned in Research Design and Methods, we addressed this discrepancy by using an equivalent RHI concentration, $[\mathrm{RHI}]_{eq}$, in IM^{3}PACT simulation, scaled from the local MK-2640 concentration, [GRI]. Through the rigorous derivation below, we found the scaling factor to be exactly the ratio of RHI and GRI IC_{50} extracted from their respective IR-binding assays. These IC_{50} values should be distinguished from those obtained from the MR-binding assays where MK-2640 and glucose compete for mannose receptors. In an IR-binding assay, a generalized antagonist ("A") competes with radio-labelled RHI molecules ("I") for insulin receptors:

$$\theta + \mathrm{I} \underset{k_{-3}}{\overset{k_3}{\rightleftharpoons}} \theta_{\mathrm{I}} \xrightarrow{k_4} \theta + \mathrm{P} \tag{S1}$$

$$\theta + \mathrm{A} \underset{k_{-5}}{\overset{k_5}{\rightleftharpoons}} \theta_{\mathrm{A}} \xrightarrow{k_4} \theta \tag{S2}$$

The extent of competitive binding can be quantified by measuring the signal of P, the product derived from bound radio-labelled RHI. With the same quasi-steady-state assumption as in Equation 3, we derive:

$$\frac{d\theta_{\mathrm{I}}}{dt} = k_3\theta[\mathrm{I}] - \left(k_{-3} + k_4\right)\theta_{\mathrm{I}} = 0 \tag{S3}$$

The same can be carried out for $d\theta_A/dt$ based on Equation S2. We therefore relate the concentrations of free (θ), RHI-bound (θ_I), and antagonist-bound IR sites (θ_A) by:

$$\begin{cases} \theta_{\mathrm{I}} = \dfrac{k_3\theta[\mathrm{I}]}{k_{-3} + k_4} = \dfrac{\theta[\mathrm{I}]}{K_{\mathrm{I}}} \\ \theta_{\mathrm{A}} = \dfrac{k_5\theta[\mathrm{A}]}{k_{-5} + k_4} = \dfrac{\theta[\mathrm{A}]}{K_{\mathrm{A}}} \end{cases} \tag{S4}$$

where $K_I = (k_{-3} + k_4) / k_3$ and $K_A = (k_{-5} + k_4) / k_5$. Given $\theta_I + \theta_A + \theta = \theta_{tot}$, we are able to obtain an expression for θ_I dependent only on known variables:

$$\theta_{\mathrm{I}} = \frac{\theta_{\mathrm{tot}}[\mathrm{I}]}{[\mathrm{I}] + K_{\mathrm{I}}[\mathrm{A}] / K_{\mathrm{A}} + K_{\mathrm{I}}} \tag{S5}$$

In a control experiment where the antagonist is absent, θ_I is obviously:

$$\theta_{\mathrm{I,\,max}} = \frac{\theta_{\mathrm{tot}}[\mathrm{I}]}{[\mathrm{I}] + K_{\mathrm{I}}} \tag{S5}$$

When $[A] = [A]_{IC50}$, therefore, θ_I is by definition half of $\theta_{I,\,max}$:

$$\theta_{\mathrm{I,\,IC50}} = \frac{1}{2}\frac{\theta_{\mathrm{tot}}[\mathrm{I}]}{[\mathrm{I}] + K_{\mathrm{I}}} = \frac{\theta_{\mathrm{tot}}[\mathrm{I}]}{[\mathrm{I}] + K_{\mathrm{I}}[\mathrm{A}]_{\mathrm{IC50}} / K_{\mathrm{A}} + K_{\mathrm{I}}} \tag{S6}$$

In other words,

$$[\mathrm{A}]_{\mathrm{IC50}} = \frac{K_{\mathrm{A}}}{K_{\mathrm{I}}}[\mathrm{I}] + K_{\mathrm{A}} \tag{S7}$$

Since the derivation does not depend on specific antagonist used in the assay, the species A may represent either MK-2640 (the "GRI"), or simply RHI molecules which compete with their labelled counterparts. We derive the corresponding IC_{50} expressions from Equation S7:

$$[\mathrm{RHI}]_{\mathrm{IC50}} = [\mathrm{I}] + K_{\mathrm{I}} \tag{S8}$$

$$[\mathrm{GRI}]_{\mathrm{IC50}} = \frac{K_{\mathrm{A}}}{K_{\mathrm{I}}}[\mathrm{I}] + K_{\mathrm{GRI}} \tag{S9}$$

where K_{GRI} is the K_A for MK-2640. Incidentally, we notice the ratio of the IC_{50} values is exactly:

$$\frac{[\mathrm{RHI}]_{\mathrm{IC50}}}{[\mathrm{GRI}]_{\mathrm{IC50}}} = \frac{K_{\mathrm{I}}}{K_{\mathrm{GRI}}} \tag{S10}$$

Since the glucose-lowering effect of insulin and MK-2640 takes place with bound IRs as an intermediary, we can define $[RHI]_{eq}$ as the concentration of RHI that yields the same θ_I as the θ_{GRI} resultant from a certain local MK-2640 level.

$$\theta_{\mathrm{GRI}} = \frac{[\mathrm{GRI}]}{K_{\mathrm{GRI}}}\theta = \frac{[\mathrm{RHI}]_{\mathrm{eq}}}{K_{\mathrm{I}}}\theta = \theta_{\mathrm{I}} \tag{S11}$$

Therefore,

$$\begin{aligned}[\mathrm{RHI}]_{\mathrm{eq}} &= [\mathrm{GRI}]\frac{K_{\mathrm{I}}}{K_{\mathrm{GRI}}} \\ &= [\mathrm{GRI}]\frac{[\mathrm{RHI}]_{\mathrm{IC50}}}{[\mathrm{GRI}]_{\mathrm{IC50}}}\end{aligned} \tag{S12}$$

given Equation S10. The simple yet exact relation in Equation S12 allows us to use the physiological model developed for RHI for MK-2640 simulation. The IR IC_{50} values for both RHI and MK-2640 have been experimentally determined *in vitro* for humans, minipigs, and dogs.[14] When we used these respective *in vitro* IC_{50} as initial guesses for MK-2640's *in vivo* relative IR affinities (see Table 1), the parameterized values deviated very little from the *in vitro* ratios.

S3. Supplementary Figures

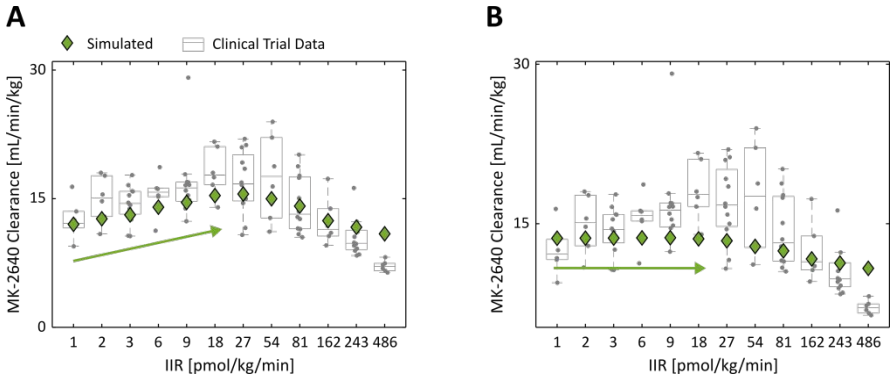

Figure S1. A cooperative Hill coefficient hGRI is necessary to capture the initial rise in MK-2640 clearance at lower IIRs as reported in Trial 1 clamp study of MK-2640.[4] This is evident by contrasting the simulated clearances with $h_{GRI} = 1.5$ (*A*) and $h_{GRI} = 1$ (*B*). In both panels, $h = 2.537$ and $K_M = 3.4$. K_G was adjusted to 1.41E-2 in panel *B* to match the *in vitro* inhibition curve. The arrows serve as guides for the eye. Given the lack of binding assay data with varying concentrations of MK-2640 at a fixed [G], hGRI of 1.5 was instead inferred by fitting with the Krug et al.'s clinical clamp studies of escalating MK-2640 infusion rates.[4] The need for a cooperative hGRI larger than unity is clear, however, even before we attempted to quantitatively fit the model, being (i) evident from the significant initial rise in MK-2640 clearance with increasing concentrations, and (ii) consistent with literature on insulin-receptor binding.

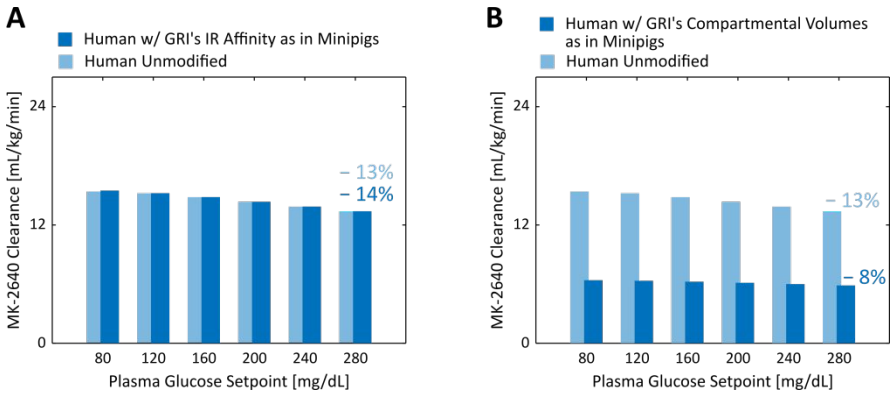

Figure S2. MK-2640 parameters found to not have contributed to the clinical underperformance despite their significant interspecies differences in minipigs and humans (*cf.* Figure 4F, G, also see Table 1). *A*: A modulation of 14% was observed if the same MK-2640 IR affinity was simulated in humans as in minipigs, which was a minimal improvement from the base case (13%). *B*: If MK-2640's compartmental volumes in minipigs were used for the human physiological model, the change in GRI clearance would be even worse (8%) than the base case scenario.

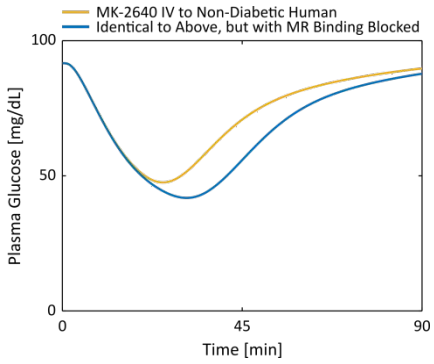

Figure S3. Simulated plasma glucose response to an intravenous dose of MK-2640 in a non-diabetic human, with (yellow) and without (blue) competitive clearance by MR. While the difference between the two scenarios is smaller than in a non-diabetic minipig (see Figure 3B), it was evident that MR-mediated clearance was not completely shut off under eu- and hypoglycemic conditions in humans. The MK-2640 dose was selected to be 4.85nmol/kg, scaled from the RHI dose of 0.17nmol/kg[14] by the same factor used in the clinical trial.[4]

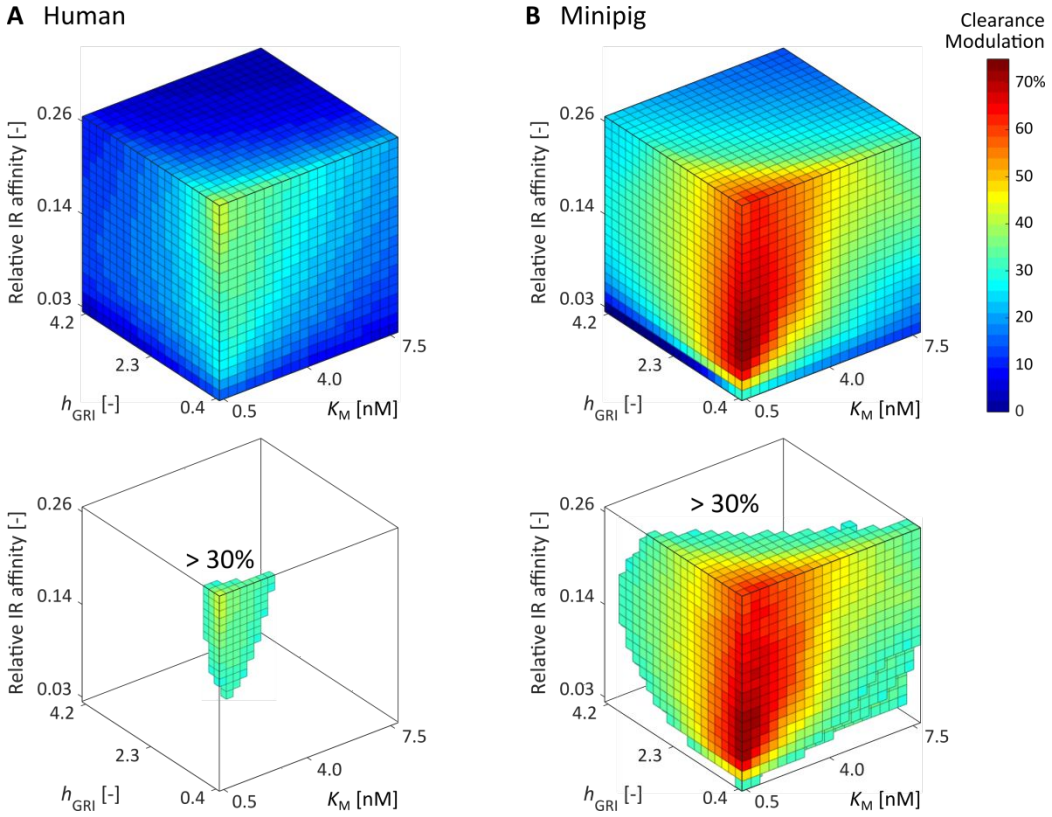

Figure S4. Simulated changes in clearance between eu- and hyperglycemic clamps at 90 and 300 mg/dL for competitive clearance GRI candidates spanning a design space expanded from that in Figure 5. Even with wider parameter ranges, only a minimal set of parameter combinations translates to a clearance modulation above 30% in humans (*A*), in stark contrast to the minipig simulations (*B*).

S4. References

1. Brown LD, Liu J, Shoemake C, Brocksmith D, Trickey J, Teel A. Miniature Swine Book of Normal Data. 2019.

2. Wyler F, Käslin M, Hof R, Beglinger R, Becker M, Stadler G, et al. Das Göttinger Miniaturschwein als Versuchstier - 5. Mitteilung: Das Herzminutenvolumen, seine prozentuale Verteilung auf den Organismus und die effektive Organdurchblutung. Research in Experimental Medicine [Internet]. 1979 Feb;175(3):31–6. Available from: http://link.springer.com/10.1007/BF01851231

3. Sorensen JT. A physiologic model of glucose metabolism in man and its use to design and assess improved insulin therapies for diabetes. Massachusetts Institute of Technology; 1985.

4. Krug AW, Visser SAG, Tsai K, Kandala B, Fancourt C, Thornton B, et al. Clinical evaluation of MK-2640: An insulin analog with glucose-responsive properties. Clin Pharmacol Ther. 2019 Feb 30;105(2):417–25.

5. Suenderhauf C, Parrott N. A physiologically based pharmacokinetic model of the minipig: Data compilation and model implementation. Pharm Res. 2013;30(1):1–15.

6. Lunze K, Woitok A, Walter M, Brendel MD, Afify M, Tolba R, et al. Analysis and modelling of glucose metabolism in diabetic Göttingen minipigs. Biomed Signal Process Control [Internet]. 2014;13(1):132–41. Available from: http://dx.doi.org/10.1016/j.bspc.2014.04.003

7. Chandrasena LG, Fettman MJ, Hand MS. Endotoxin dose. II. Effects on glucose biokinetics in Yucatan minipigs. Am J Physiol Endocrinol Metab. 1983;7(4).

8. Muller MJ, Paschen U, Seitz HJ. Glucose production measured by tracer and balance data in conscious miniature pig. American Journal of Physiology-Endocrinology and Metabolism [Internet]. 1983 Mar 1;244(3):E236–44. Available from: https://www.physiology.org/doi/10.1152/ajpendo.1983.244.3.E236

9. Sanguinetti E, Liistro T, Mainardi M, Pardini S, Salvadori PA, Vannucci A, et al. Maternal high-fat feeding leads to alterations of brain glucose metabolism in the offspring: positron emission tomography study in a porcine model. Diabetologia. 2016;59(4):813–21.

10. Murphy JR. Erythrocyte metabolism. II. Glucose metabolism and pathways. J Lab Clin Med [Internet]. 1960 Feb;55:286–302. Available from: http://www.ncbi.nlm.nih.gov/pubmed/14425397

11. Bakh NA, Bisker G, Lee MA, Gong X, Strano MS. Rational design of glucose-responsive insulin using pharmacokinetic modeling. Adv Healthc Mater. 2017;6(22):1–10.

12. Wong J, Chase JG, Hann CE, Shaw GM, Lotz TF, Lin J, et al. A subcutaneous insulin pharmacokinetic model for computer simulation in a diabetes decision support role: Model structure and parameter identification. J Diabetes Sci Technol. 2008;2(4):658–71.

13. Wong J, Chase JG, Hann CE, Shaw GM, Lotz TF, Lin J, et al. A subcutaneous insulin pharmacokinetic model for computer simulation in a diabetes decision support role: Validation and simulation. J Diabetes Sci Technol. 2008 Jul;2(4):672–80.

14. Kaarsholm NC, Lin S, Yan L, Kelly T, van Heek M, Mu J, et al. Engineering glucose responsiveness into insulin. Diabetes. 2018;67(2):299–308.

15. Yang JF, Gong X, Bakh NA, Carr K, Phillips NFB, Ismail-Beigi F, et al. Connecting rodent and human pharmacokinetic models for the design and translation of glucose-responsive insulin. Diabetes [Internet]. 2020 Aug 9;69(8):1815–26. Available from: http://diabetes.diabetesjournals.org/lookup/doi/10.2337/db19-0879